Experimental and Numerical Investigation of the Electro-Mechanical Response of Particle Filled Elastomers - Part I: Experimental Investigations

Markus Mehnert, Jessica Faber, Mokarram Hossain, Shawn A. Chester and Paul Steinmann

Abstract Electro-active polymers (EAPs) have the ability to undergo large deformations upon the stimulation by an electric field. They offer new design possibilities in a variety of applications, such as simple soft and flexible actuators, stretchable sensors, and energy harvesters. In the subclass of dielectric elastomers, the operation principle relies on the Coulomb forces between charged electrodes that deform the soft polymer. As the forces are dependent on the permittivity of the dielectric, the addition of filler particles with a high permittivity is a promising approach to increase the overall electro-mechanical coupling. This contribution presents the results of various mechanical and electro-mechanical experiments conducted with the silicone Elastosil P 7670^{TM} filled with Barium-Titanate particles. These experiments are performed in such a fashion that the obtained results are well suited for the identification of the necessary material parameters of an electro-viscoelastic modelling approach in Part II of this contribution (Mehnert et al. Submitted).

Markus Mehnert
Institute of Applied Mechanics, University of Erlangen-Nuremberg, Egerlandstr. 5, 91058 Erlangen, Germany, e-mail: markus.mehnert@fau.de

Jessica Faber
Institute of Applied Mechanics, University of Erlangen-Nuremberg, Egerlandstr. 5, 91058 Erlangen, Germany, e-mail: jessica.faber@fau.de

Mokarram Hossain
Zienkiewicz Centre for Computational Engineering, College of Engineering, Bay Campus, Swansea University, Swansea, UK e-mail: mokarram.hossain@swansea.ac.uk

Shawn A. Chester
Mechanical & Industrial Engineering Department, New Jersey Institute of Technology, 200 Central Ave., Newark, NJ 07102, USA, e-mail: shawn.a.chester@njit.edu

Paul Steinmann
Institute of Applied Mechanics, University of Erlangen-Nuremberg, Egerlandstr. 5, 91058 Erlangen, Germany e-mail: paul.steinmann@fau.de
Glasgow Computational Engineering Centre (GCEC), University of Glasgow, United Kingdom

1 Introduction

In view of the increasing importance of the rubber industry since the 1950s, special requirements have been made ever since on the material behavior of elastomers for technical applications [1]. Filler materials such as carbon black, silica or Barium-Titanate particles are often used to optimize the physical and mechanical properties and to increase electrical permittivity of the resulting compound [2, 3, 4]. The influence of fillers depends on the type, shape, and quantity and their interaction is complex in nature [5, 6]. A material class in which the addition of filler particles shows a great potential are the so-called dielectric elastomers (DEs), which form a subset of electro-active polymers (EAPs). They have the capability to undergo large deformations upon the stimulation by an electric field. The simplest form of a soft actuator made of dielectric elastomeric material consists of a thin dielectric layer sandwiched between two compliant electrodes. In such a configuration, the electrodes serve as the plates of a capacitor whereas the filled polymer is the dielectric medium. The high permittivity of the filler material increases the overall permittivity of the compound, effectively reducing the voltage required for the actuation.

The synthesis of dielectric elastomer composites filled with high dielectric constant fillers to improve dielectric and electromechanical properties has been an active field of research over the past decade. Pioneering is the work of Carpi et al. [7], in which a Titanium-Dioxide powder was dispersed in a silicone matrix enabling a significant reduction of the driving electric field. More recently, Ruan et al. [8] filled butyl rubber with 30 wt.% of Barium-Titanate particles to increase the dielectric constant from 2.8 to 3.7 resulting in an increase of the actuation strain induced by an electric field by a factor of 7. Yang et al. [9] synthesised widely used natural rubber-based polymer composites in which Titanium-Oxide is used as a high dielectric permittivity ceramic filler. In this case, they achieved an enhanced dielectric permittivity with surface modified fillers. In contrast to traditional natural rubbers, Yin et al. [10] used polyurethane (PU) as the base polymer and filled it with Barium-Titanate fillers. They successfully synthesized and experimentally obtained PU-based dielectric elastomers in which the dielectric constant is increased more than 50% for an addition of fillers with 50% by weight. As an alternative filler material, Jose et al. [11] presented experimental studies performed with a combination of natural rubber and carbon nanotubes (CNT) resulting in an enhancement of mechanical properties of the compound. This, however, comes at the cost of a simultaneous decrease in the dielectric breakdown strength [12].

Recently, the effects of high permittivity fillers on the response of silicones were investigated in an experimental study by Kumar et al. [13]. Therein, a composite of silicone and Barium-Titanate filler was cured in the presence of an electric field resulting in an improvement of the electromechanical properties. Furthermore, investigations on the influence of the size of the particles and a detailed analysis of their effects on the dielectric breakdown strength were presented in the works of Ziegmann et al. [14, 15]. The aforementioned works put their primary focus on the

syntheses of the materials and the resulting effects of the addition of stiff filler particles. Similarly, Huang et al. achieved excellent dielectric responses in experiments with an electro-active polymer nanocomposite consisting of polyurethane and high dielectric constant copper phtalocyanince oligomer particles [16]. The material was produced using a combination of top down and bottom up approaches that enabled extremely high electromechanical responses, resulting in field induced strains of more than 8 %, with low volume fractions of fillers (~ 3.5 vol.%). Moreover, the dielectric constant of these compounds was analyzed taking the frequency dependence of the applied electric field into account and those were compared to simple blends of the same material combination and the unfilled matrix.
However, the data presented is not obtained with the goal of providing information for a computational modelling framework that is the basis for a numerical simulation of the EAP composite materials. This necessitates a separate and detailed investigation of the effects of the filler particles on the elastic and viscous material response as well as the electro-mechanical behavior of the compound.

Consequently, in the current work, we present an extensive investigation of the silicone Elastosil P 7670^{TM} filled with Barium-Titanate particles. The material is experimentally characterized under mechanical and electro-mechanical loadings. All of the experiments are performed in such a way that the obtained data is well suited for a subsequent parameter identification as a basis of a computational modelling framework. Therefore, we perform a modular investigation so that the different experiments allow for a distinction between the individual material characteristics, i.e., purely mechanical multistep relaxation experiments for the characterization of the elastic material response, purely mechanical cyclic loading tests for the identification of the viscous material response and experiments with an applied electric field for the identification of the electro-mechanical coupling parameters.

This contribution is structured as follows: in Sections 2 and 3 the testing equipment and the sample preparation are described in detail followed by the results of the conducted experiments, summarized in Section 4. The contribution is concluded by a short outlook.

2 Experimental Setup

Experiments were performed on two different machine setups. In the case of the mechanical tests, a single-spindle testing machine *Inspekt S 5 kN* by Hegewald & Peschke was used as depicted in Figure 1. The device consists of a control unit (1) situated in a separate case, a rigid aluminum test frame (2), a single-spindle load unit driven by an AC servomotor (3), bellow seals (4) that protect the single spindle against any dirt or possible oil leakage, a force transducer (R-load cell 5 kN, Hegewald & Peschke) (5). The device is combined with a temperature chamber *T54 LN2* by Mytron that was used for the additional thermal experiments. The machine is

connected to a local compressed air supply system. Thus, the material sample can be mounted into the testing device using pneumatically activated clamps (9) controlled via foot pedals (10). The force transducer calculates the measured force with a standard deviation of ± 0.01 (calibration class 1 acc. to DIN EN ISO 7500), converts it into an electrical signal and sends it to the connected PC for data acquisition. Due to the internal dimensions of the thermo chamber, the maximum displacement of the single-spindle is restricted to 350 mm at a traverse speed of up to 33 mm/s.

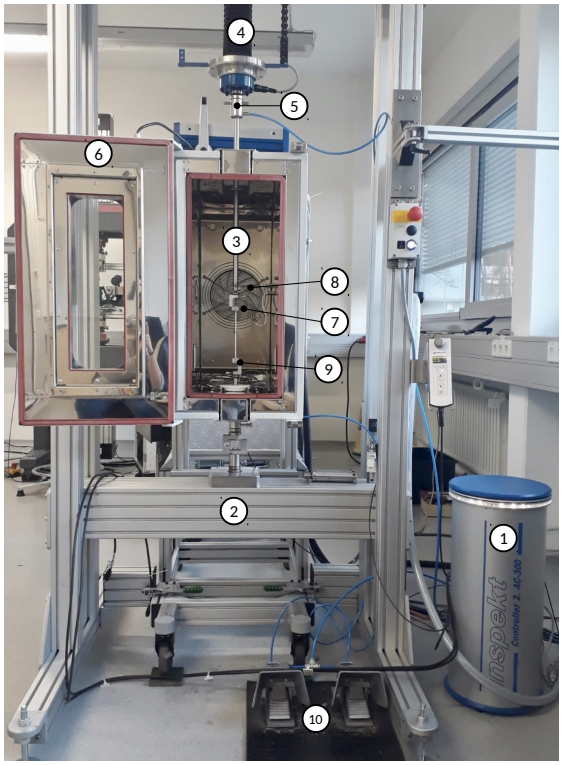

Fig. 1 Deformed state material sample mounted in the single-spindle testing machine Hegewald & Peschke *Inspekt S 5 kN*. *Legend:* **1** control unit, **2** aluminum test frame, **3** single-spindle load unit, **4** bellow seals, **5** force transducer, **6** temperature chamber, **7** integrated fan, **8** temperature sensors, **9** pneumatic clamps, **10** foot pedals.

As the *Inspekt 5 kN* is not equipped for the application of high electric voltages on the material samples, the electro-mechanical experiments were performed on a custom-made testing device. The setup, as depicted in Figure 2, consists of ten major parts, including a temperature regulation system that is not used during the experiments presented in this context. The material sample (**1**) is mounted in the machine at both

ends by a pair of clamps (**2**). The bottom pair is fixed at the bottom of the thermo chamber (**3**), while the top plates are connected to the linear stage (**4**) via a 300 mm long rod. The rod is placed through a hole at the top of the thermo chamber and is connected to the linear stage via the force transducer (**5**) (model number GSO-1 K, Transducer Techniques) that in turn is connected to the frame of the testing system (**6**). The bottom clamps are designed with a metallic connector for the electric wiring that is directly attached to the sample. As the material is stretched upwards and the bottom clamps are fixed, the wiring (**7**) does not move during the deformation of the material which establishes the connection between the sample and the electric voltage supply (**8**). The latter is visible in the right part of Figure 2 placed on top of the thermal control unit (**9**). In order to ensure work safety, a non-conductive cabinet (**10**) encloses the entire setup. Over the course of the deformation, the applied force is constantly recorded with a frequency of 10 data points per second. The force transducer (precision limit of ±0.01 g) is connected to a PC with a custom-made LabView system.

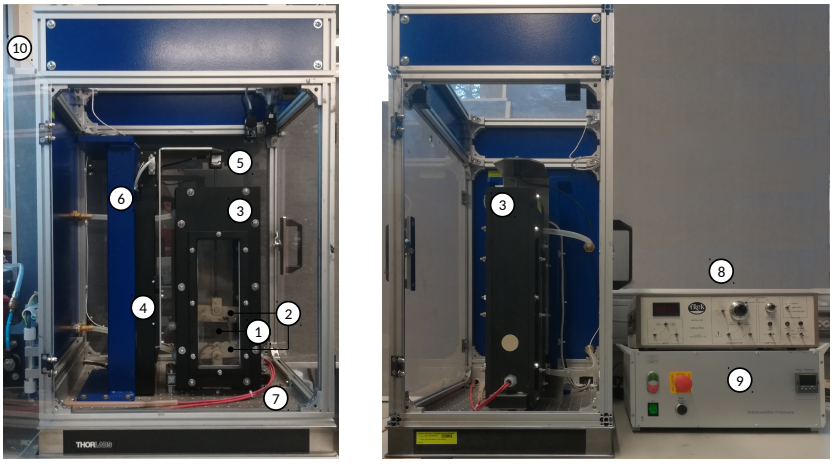

Fig. 2 Coated test sample mounted inside the thermal chamber depicted in (left) side view and (right) front view. *Legend:* **1** coated test sample, **2** clamping plates, **3** thermo chamber, **4** linear stage, **5** force transducer, **6** frame, **7** electric wiring, **8** high voltage supply, **9** thermal control unit, **10**.

The data obtained for the experiments under consideration is presented in the following sections by plotting the resulting force over the applied stretch in which the force is directly measured by the load cell during the tests. This comes with the downside that the results of the experiments conducted with different sized cross sections can not be directly compared, as the resulting force depends on the cross section area. In the case of the mechanical tests, this could potentially be solved by transferring the measured force to an appropriate stress measure, as it is assumed that, due to the

selected dimensions of the samples, the deformation state and the resulting stress in the middle of the specimen is constant. However, in the experiments involving an electric field, the dimensions of the material sample do not allow for a direct conversion of the measured force to a single stress quantity, as the stress distribution can not be considered to be homogeneous. Thus, for the sake of consistency, we choose to keep the selected format of plotting the resulting force and scale the respective results, when a comparison between experiments with different sized cross sections is required.

3 Sample Preparation

The test samples are produced using a two-component silicone rubber Elastosil P 7670^{TM} supplied by WACKER^{TM} with a varying filler content of $BaTiO_3$ particles of sizes <2 μm, purchased from SIGMA-ALDRICH^{TM}. It should be noted here that the particles were used as received without an additional preparation, such as coating. Furthermore, no investigations on the influence of the size of the particles or on their effect on the breakdown strength are performed within the scope of the current work. For this, the interested reader is referred to the works of Ziegmann et al. [14, 15]. For the preparation of the samples, component *A* of the Elastosil and the Barium-Titanate powder are mixed homogeneously with a rotational speed of 1000 rpm to 2000 rpm for eight minutes in a speedmixer. Due to heat generation during the mixing process, the compound has to be cooled before component *B* of the Elastosil is added, otherwise undesired curing of the polymer would initiate. Once the mixture has cooled down to room temperature, the second component of the silicone is added in a ratio of 1:1.

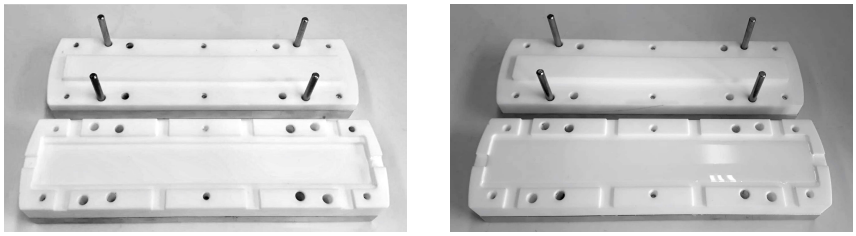

Fig. 3 (left) unfilled and (right) filled sample molds used for the preparation of silicone samples intended for mechanical testing.

Homogeneity in the polymeric composite is achieved by mixing the material in the speedmixer at 1000 rpm for one minute. Subsequently, the compound is poured into a suitable mold. For the mechanical experiments, material samples with the thickness of 1.7 mm and the in-plane dimensions 260 mm by 35 mm are produced (Figure 3). In the case of electro-mechanical experiments, material samples with different dimensions are required, i.e., the thickness of the specimens has to be as small as possible

while the in-plane dimensions have to be increased. Therefore, molds are selected that can produce material samples with a thickness of 0.7 mm and the in-plane dimensions 115 mm by 115 mm (Figure 4). To avoid the inclusion of air bubbles, the filled molds are put into a desiccator with a connected vacuum pump for up to ten minutes, cf. Figure 5 until the formation of bubbles on the material surface has ceased to exist.

Fig. 4 unfilled sample molds used for the preparation of silicone samples intended for electromechanical testing.

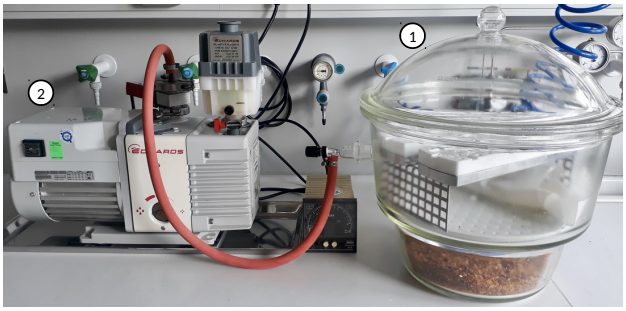

Fig. 5 Desiccator (1) with connected vacuum pump (2) used for the preparation of the silicone samples in order to extract air bubbles from the material samples.

Subsequently, the material samples are allowed to cure inside closed molds. Even though this silicone is a room temperature vulcanizing polymer, the molds are placed inside an oven for one hour at 120 °C. Such a procedure results in a faster crosslinking of the silicone monomers when compared to the curing at room temperature.

Therefore, it can be assumed that the mechanical properties of the silicone are less likely to change over time. After the heating time, the material cools down inside the mold for 24 hours at room temperature. For the characterization of the material response, specimens of unfilled silicone and filled silicone with concentrations of 10 wt.%, 20 wt.%, 33 wt.% and 50 wt.% are prepared. The reader should note that, as the density of the Barium-Titanate is almost six times higher compared to the one of silicone, this results in a filling of the material of approximately 1.6 vol.%, 3.3 vol.% 5.5 vol.% and 9 vol.%. As the volume percentage is the main parameter for the simulation, it will be used for the presentation and the discussion of the obtained results.

To ensure that the particles inside the silicone matrix are distributed homogeneously without conglomerations, the morphology of the compound is investigated using a Scanning Electron Microscope (SEM). To this end, material samples are initially bi-sected using cryofracture, i.e., the samples are cooled down below the glass transition temperature by immersion into a liquid nitrogen and afterwards broken using two nitrogen-cooled pliers. Thus, a cross section of the material is generated without the risk of undesired effects from cutting. To increase the image contrast obtained from the SEM, an electrically conductive layer of gold is sputtered onto the cross section. Figure 6 shows the SEM image of a silicone sample with 8.3 vol.% Barium-Titanate.

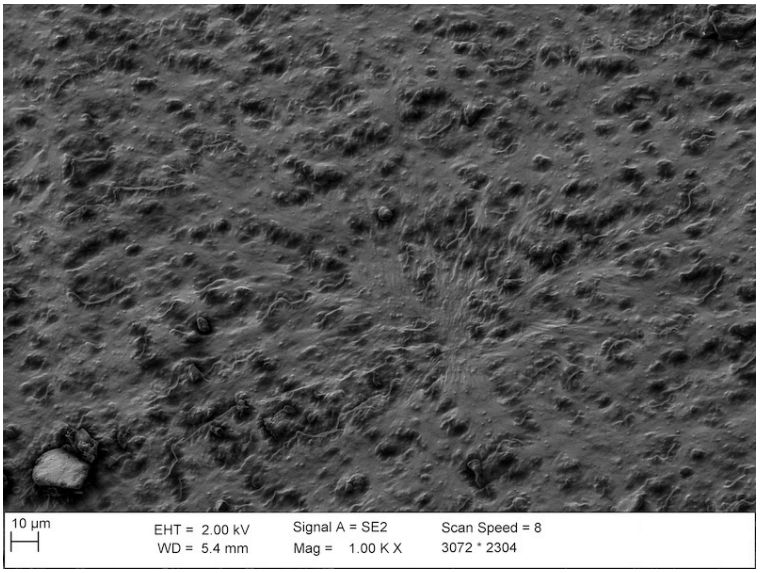

Fig. 6 Particle distribution for filled silicones with 8.3 vol.% $BaTiO_3$. Filler particles appear in black, silicone matrix is grey.

The $BaTiO_3$ particles appear in black, whereas the silicone matrix is grey. The particles show a homogeneous distribution throughout the material without any

accumulations, which is a prerequisite for the intended material characterization. In the following section, the conducted experiments are described in detail, starting with the characterization of the mechanical material response for pure Elastosil and for the particle filled compound with various filler concentrations.

4 Experimental results

The following sections present the results of the conducted experiments that follow the same protocol as in the case of experiments on VHB 4905^{TM}, a very similar material, which was published in a preceding contribution [17]. At first, experiments were carried out to identify the influence of the so-called Mullins effect. However, it was not observed and will therefore not be considered in the following sections. Furthermore, an investigation of the influence of changes in the material temperature ranging from room temperature to 100 °C was also conducted but no significant effect of temperature on the material response was observed. Thus, no thermo-mechanical experiments are presented within the scope of the current work.

4.1 Multi-Step Relaxation Tests

The multi-step relaxation tests follow the same protocol as in our prior work [17], i.e., the test samples are stretched in steps of 25% at a deformation rate of 30 mm/s up to a maximum stretch of 200 %. Each step is followed by a relaxation period of 30 minutes. We assume that the material has reached a state very close to the equilibrium stress after the holding period of 30 minutes. The reader should note that longer holding periods would approximate the configuration in which the polymer chains are completely relaxed more precisely. Such an increase in the holding period however is not practical for multistep relaxation experiments with the aim of performing the tests multiple times to ensure reproducibility. Moreover, in a wide range of practical applications, the deformation rates lead to a clear dominating role of the viscous material response and thus a holding period of thirty minutes is considered as sufficient in the scope of the current work. These tests are performed at room temperature on five material samples for each filler concentration to ensure reproducibility. As the material is custom-made, the deviation of each test is potentially larger than compared to the commercially available materials. Therefore, Figure 7 shows typical results and the average of the multistep relaxation tests for five samples with 8.3 vol.% $BaTiO_3$ fillers. The average curve is depicted as a thick black line.

Clearly, despite the best efforts, the results of the five multi-step relaxation tests deviate from each other. However, due to the complex manufacturing process of the

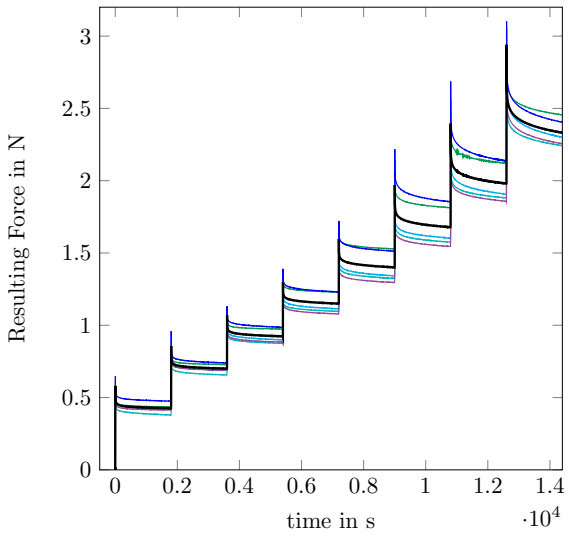

Fig. 7 Resulting force over time of multi-step relaxation tests of five samples with 8.3 vol.% of $BaTiO_3$ and a deformation rate of 30 mm/s. Average result depicted as thick black line.

material and the manual cutting of the samples, it is almost impossible to reduce these differences with the available equipment. In Figure 8 a comparison between the results of multi-step tests with various filler contents is depicted. The left plot shows the resulting force over time for the entire experiment for unfilled Elastosil and the maximum filler concentration of 8.3 vol.%. The plot on the right-hand side shows the equilibrium curves of all selected filler concentrations.

The material response changes significantly due to the addition of $BaTiO_3$ particles. In both plots of Figure 8, it is clearly visible that the material becomes stiffer with an increase in filler content, thus the resulting force increases. For the maximum applied stretch, this increase of the resulting force in the equilibrium state between the unfilled silicone and the material with 8.3 vol.% filler concentration is more than 50 %. Furthermore, the viscous material response is influenced by the addition of particles as well. This is reflected in the more pronounced overstress and more distinct relaxation behavior in the case of 8.3 vol.% when compared to the response of pure Elastosil, depicted in the left plot of Figure 8.

4.2 Cyclic Loading Tests

The cyclic loading tests performed with silicone samples follow the same protocol as in the case of VHB 4905^{TM} [17]. Initially, the material is deformed at a constant

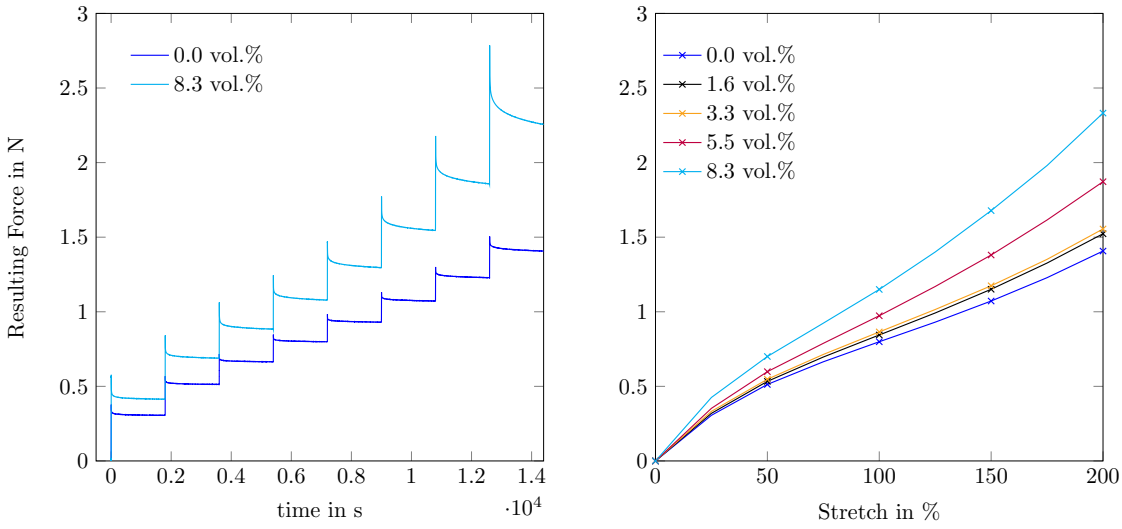

Fig. 8 (left) Average of the resulting force over time of multi-step relaxation tests for pure Elastosil and samples with 8.3 vol.% of $BaTiO_3$. (right) Resulting equilibrium curves for all tested filler concentrations.

stretch rate up to a maximum stretch of 200 %. Once the maximum deformation is reached, it is instantly reduced with the same stretch rate, until the testing device returns to its initial position. The material is deformed at stretch rates of 0.01 s^{-1}, 0.2 s^{-1}, 0.4 s^{-1} and 0.6 s^{-1}. Each cyclic loading test is repeated with five different material samples to ensure reproducibility. In order to provide an impression on the variation in the material response of the different samples, the force over applied stretch for each of the five individual experiments performed at a stretch rate of 0.2 s^{-1} with a filler concentration of 8.3 vol.% is depicted in Figure 9.

The individual results from the experiments with the filled silicone samples show a comparable deviation between each other similar to our prior work [17]. The resulting average of the curves can, therefore, be considered as a suited representative of the material response. Figures 10 and 11 summarize the results of the cyclic loading experiments for the filler concentrations 0 vol.%, 3.3 vol.%, 5.5 vol.%, 8.3 vol.% and all tested stretch rates.

The pure silicone shows a response that should be noted especially for a subsequent modelling approach. A comparison between the data of the slowest stretch rate ($\dot{\lambda} = 0.01$ s^{-1}) and the result of the multistep relaxation test shows that the loading curve is almost identical to the equilibrium curve. Thus, the slowest cyclic loading

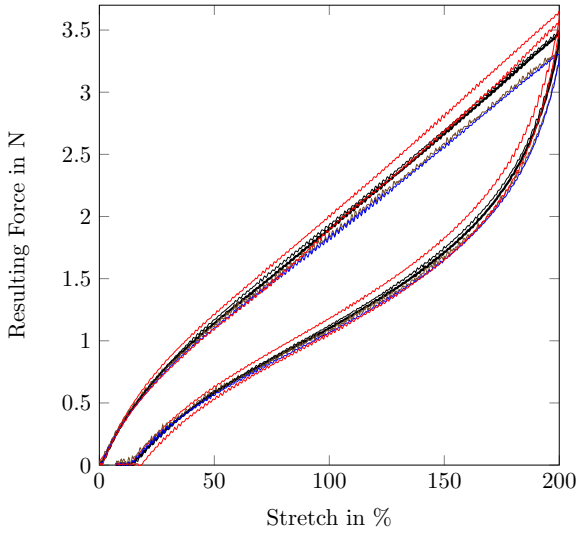

Fig. 9 Resulting force over the applied stretch of cyclic loading tests of five samples with 8.3 vol.% of $BaTiO_3$ and a stretch rate of 0.2 s^{-1}.

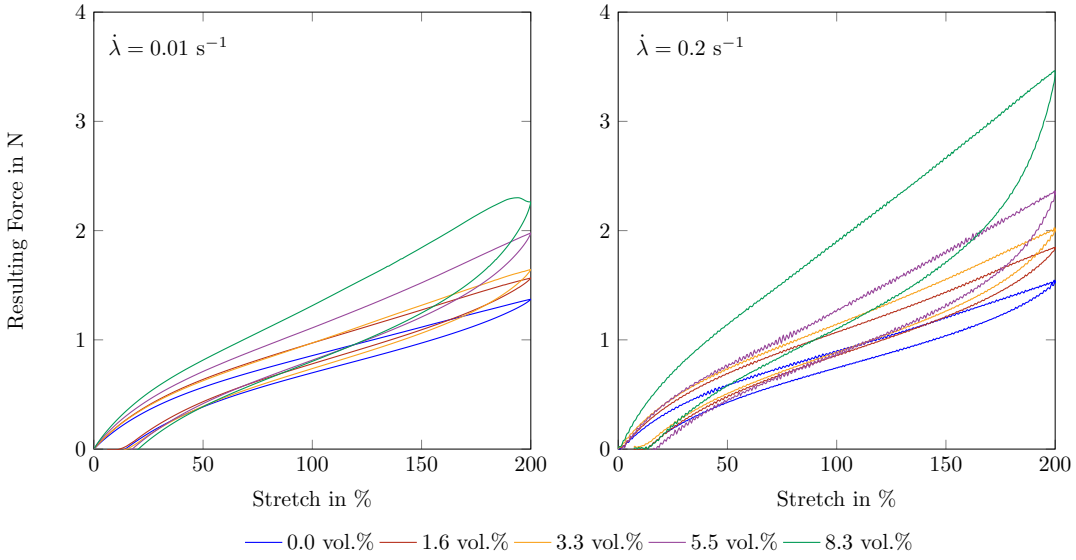

Fig. 10 Resulting force over the applied stretch of cyclic loading tests with various filler concentrations and a stretch rate of (left) 0.1 s^{-1} and (right) 0.2 s^{-1}.

test can be considered as the elastic (quasi-static) response of the material. Due to this assumption, no further experiments with slower strain rates are performed. However, as the unloading path does not follow the loading path a hysteresis curve is visible

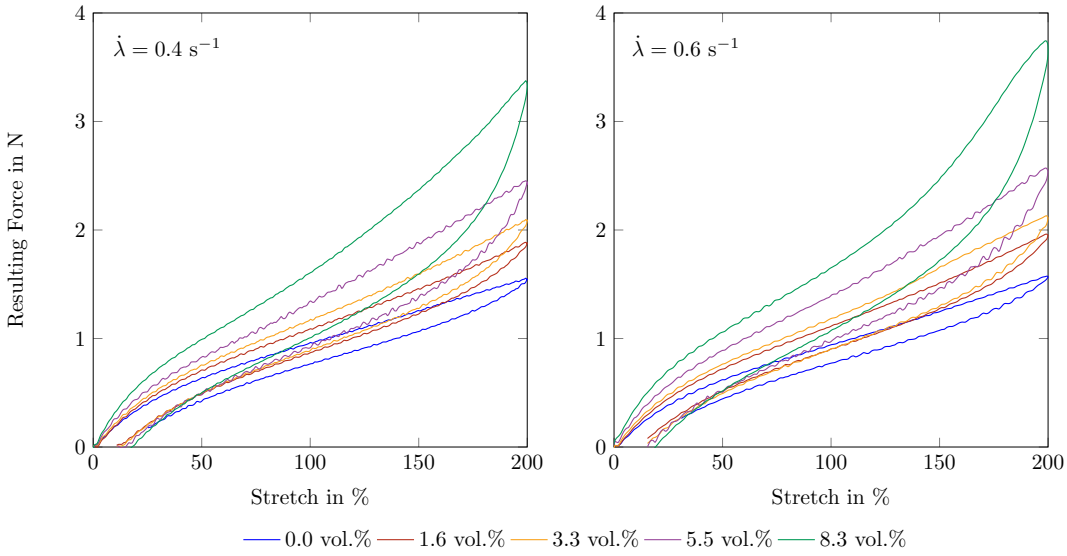

Fig. 11 Resulting force over the applied stretch of cyclic loading tests with various filler concentrations and a stretch rate of (left) 0.4 s^{-1} and (right) 0.6 s^{-1}.

that can not be attributed to the Mullins effect, which had been excluded by prior experiments. Therefore, as shown in the subsequent publication on the modelling approach, the concept of pseudo-elasticity [18, 19] is adopted to fit the observed material responses.

Upon the addition of particles, the general response of the material is altered, e.g., the viscous responses increase with an increase in the filler concentration. The change in viscous behavior is demonstrated both by the enlargement of the hysteresis curves and by an increase in the rate-dependency for material compositions with a higher concentration of $BaTiO_3$ particles. This enhanced viscous material response can be explained by energy dissipations inside the material due to frictions between the silicone and the embedded stiff particles and are in accordance with the literature [20, 21]. In order to give the reader an impression of the magnitude of this increase in dissipation, the area of the hysteresis of the pure silicone can be compared to the respective area of the filled material. As an example, the hysteresis curves obtained at 0.01 s^{-1} and 0.6 s^{-1} with 0.0 vol.%, 3.3 vol.% and 8.3 vol.% particle concentration are calculated. This reveals, that for the slowest deformation rate, the hysteresis increases from an area of 28.12 for the unfilled material, to an area of 40.66 in the case of 3.3 vol.% and an area of 90.40 for 8.3 vol.% particle concentration. This corresponds to an increase of 44 % from the unfilled material to 3.3 vol.% and an increase of 221 % from the unfilled material to 8.3 vol.% particle concentration. For the fastest deformation rate, the respective values for the unfilled and filled material are 31.76, 55.75 and 125.99, which correspond to an increase of 75 % and 296 %

respectively. These show an enormous influence that the particles have on the energy dissipation inside the material.

4.3 Electro-Mechanical Tests

The main target of adding Barium-Titanate particles to the silicone is to increase the electric permittivity of the material, potentially amplifying the response of the dielectric elastomer under the application of an electric field. The results of the mechanical tests have shown however that due to the high stiffness of the filler particles, the compound material stiffens considerably. In order to investigate the interplay of these opposing effects on the electro-mechanical response, cyclic loading tests are performed under the application of an electric potential difference in the thickness direction. For these electro-mechanical test, the produced material is cut to samples with in-plane dimensions of 10 mm by 80 mm with a thickness of 0.7 mm. The maximum applied stretch is 200 % with a fixed stretch rate of 0.1 s^{-1}. With a primary goal to determine the effect of electric field on the behavior, due to the long fabrication time and that samples can only be used once because of the conductive grease, we restrict ourselves to a single stretch rate.

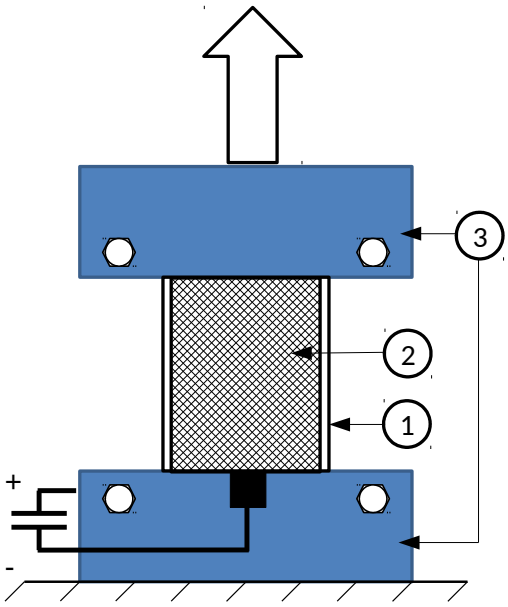

Fig. 12 Sketch of a test test sample (1) covered with electrically conductive carbon grease (2) with top and bottom clamping plates (3).

In order to induce an electric field during the cyclic loading tests, samples (**1**) are covered on both sides with electrically conductive carbon grease (**2**). As a high voltage is supplied through contacts in the clamping plates (**3**), it is especially important to ensure that the sample surface next to the clamping plates is sufficiently covered, as shown in Figure 12. These additional layers act as electrodes that are directly attached to the sample and can deform with the material during the experiments. If a voltage difference is applied between these layers, an electric field in the thickness direction of the specimen is induced effecting the force that is required for the specific deformation of the sample. Figure 13 shows the resulting force of cyclic loading tests performed with pure Elastosil with a potential difference of 0 kV and 6 kV.

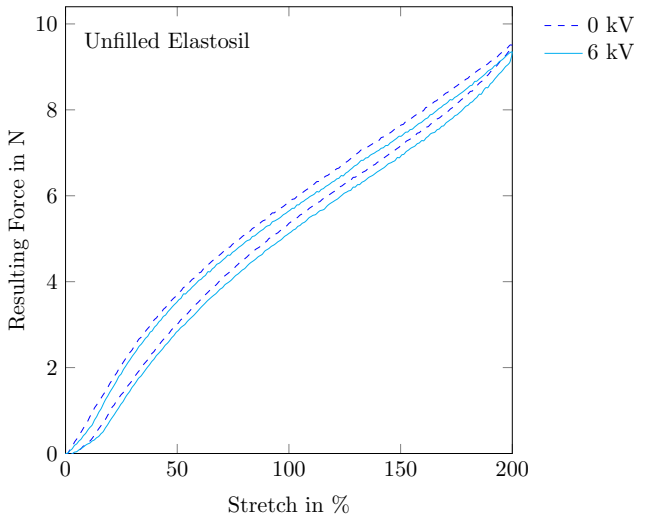

Fig. 13 Resulting force over the applied stretch of cyclic loading tests with unfilled Elastosil and a stretch rate of $0.1s^{-1}$ for electric voltage differences of 0 kV and 6 kV.

The results show a very weak effect of the electric field on the unfilled material response. When focussing on the resulting force at the maximum applied deformation, the decrease of the force is approximately 2.5 %. The results of identical cyclic loading tests for Elastosil filled with 5.5 vol.% and 8.3 vol.% of Barium-Titanate particles are presented in Figure 14. Figure 15 shows all the same results normalized to the value of the resulting force at the maximum deformation without the application of the electric field. These two plots illustrate the enhancement effect of the respective particle volume fraction upon both the hysteresis and the electro-mechanical coupling effect.

It is clearly visible that the addition of filler particles results in a significantly altered electro-mechanical response of the material. As was already explained in the mechanical investigation of the filled silicone, the silicone compounds are characterized by a stiffer response and an increase in the energy dissipation, as characterized by the increase of the size of the hysteresis. More importantly, the results in Figure 14

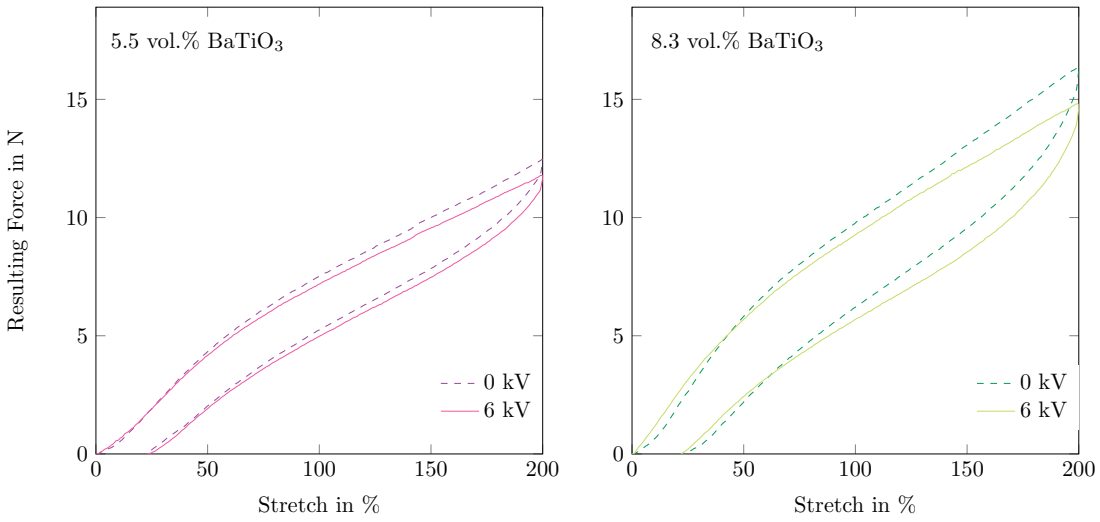

Fig. 14 Resulting force over the applied stretch of cyclic loading tests with Elastosil filled with (left) 5.5 vol.% $BaTiO_3$ and (right) 8.3 vol.% $BaTiO_3$ at a stretch rate of 0.1 s^{-1} for electric voltage differences of 0 kV and 6 kV.

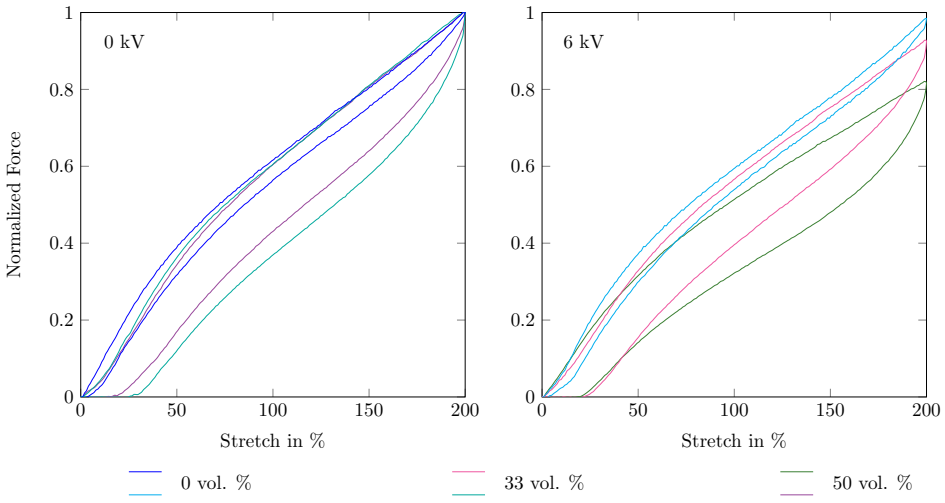

Fig. 15 Force over the applied stretch of cyclic loading tests normalized to the value of the force at the maximum deformation. (left) Normalized force for various particle concentrations withouth the application of an electric potential difference. (right) Normalized force for various particle concentrations with the application of 6 kV.

show that despite the increased stiffness of the material, the influence of the electric field on the response is significantly more pronounced for an increase in the filler concentration. When focusing on the resulting force at the maximum applied deformation, the decrease of the resulting force for a filler concentration of 5.5 vol.% $BaTiO_3$ particles is approximately 5.4 %, whereas for a filler concentration of 8.3 vol.% a reduction of 9.3 % is achieved. Consequently, it may be deduced that in the small range of tested filler concentrations, the addition of particles increases the effect of an applied electric field on the material behavior. However, this comes at the expense of an increase of the material stiffness and time dependency of the material, which has to be taken into account in the development of applications using similar material compounds. Furthermore, it should be noted that this amplification of the electro-mechanical coupling should not simply be extended to higher particle concentrations, as it has to be assumed that at a certain concentration of $BaTiO_3$ filler, the stiffer particles will dominate the material behavior, preventing a deformation of the material due to the electric field. The reader should note that a small slope at the beginning of the electro-mechanical experiments may originate from a non-straight initial configuration that could not be eliminated during the experiments.
These findings can serve as an indication to the applicability of particle filled silicones for soft electro-active actuators. It should be taken into account that, while the overall response of the material to the application of an electric field increases with increased particle concentration, the viscous characteristics of the material increase as well making the compound less suitable for high frequency applications such as flexible loudspeakers for example. However, if only the range of motion that can be achieved through the activation of the material is the deciding factor a high concentration of filler particles can lead to desirable results. A further discussion of the experimental results will also be given in Part II of this contribution that is concerned with the continuum modelling approach.

5 Summary and Outlook

In the present contribution we have experimentally investigated the electro-viscoelastic material response of the silicone Elastosil P 7670^{TM} filled with varying amounts of Barium-Titanate, high dielectric permittivity particles. For the characterization of the elastic material response, multistep relaxation tests were performed showing the stiffening effect of the filler particles. Moreover, we have presented the results of loading-unloading experiments with different stretch velocities to characterize the effects of the $BaTiO_3$ filler on the time-dependent material behavior. Finally, similar loading-unloading experiments were conducted with the application of an electric potential difference applied perpendicular to the stretch direction. The experiments have shown that the addition of filler particles lead to an enhanced effect of the electric field on the material response despite the simultaneous stiffening of the compound. All experiments were conducted in such a way that they are well suited for the identification of necessary material parameters appearing in a continuum-

based modelling approach. These simulations will be the subject of Part II of this publication series.

Acknowledgements:
M. Mehnert and P. Steinmann acknowledge the funding within the DFG project No. STE 544/52-2 and GRK2495/C. M. Hossain would like to extend his sincere appreciation to Engineering and Physical Sciences Research Council (EPSRC) for an Impact Acceleration Award (EP/R511614/1). The financial support by the Deutsche Forschungsgemeinschaft (DFG, German Research Foundation) Projektnummer 326998133 - TRR 225 (subproject B09) to J. Faber is gratefully acknowledged. S. Chester acknowledges partial support from the US National Science Foundation under grant number CMMI-1751520.

References

1. O. Stegen, *A fully micro-mechanically motivated material law for filled elastomer*. Dissertation, Gottfried Wilhelm Leibniz Universität Hannover, 2015.
2. Z. Zhang, L. Liu, J. Fan, K. Yu, Y. Liu, L. Shi, and J. Leng, "New silicone dielectric elastomers with a high dielectric constant," in *Modeling, Signal Processing, and Control for Smart Structures 2008*, vol. 6926, p. 692610, International Society for Optics and Photonics, 2008.
3. Y. Wang, J. Chen, Y. Li, Y. Niu, Q. Wang, and H. Wang, "Multilayered hierarchical polymer composites for high energydensity capacitors," *Journal of Materials Chemistry A*, vol. 7, no. 7, pp. 2965–2980, 2019.
4. L. Duan, G. L. Wang, Y. Y. Zhang, Y. N. Zhang, Y. Y. Wei, Z. F. Wang, and M. Zhang, "High dielectric and actuated properties of silicone dielectric elastomers filled with magnesium-doped calcium copper titanate particles," *Polymer Composites*, vol. 39, no. 3, pp. 691–697, 2018.
5. H. Domininghaus, P. Elsner, P. Eyerer, and T. Hirth, *Kunststoffe: Eigenschaften und Anwendungen*. Springer Heidelberg, 8. edition ed., 2012.
6. M. Stommel, M. Stojek, and W. Korte, *FEM zur Berechnung von Kunststoff- und Elastomerbauteilen*. Carl Hanser München, 2. edition ed., 2018.
7. F. Carpi and D. D. Rossi, "Improvement of electromechanical actuating performances of a silicone dielectric elastomer by dispersion of titanium dioxide powder," *IEEE Transactions on Dielectrics and Electrical Insulation*, vol. 12, no. 4, pp. 835–843, 2005.
8. M. Ruan, D. Yang, W. Guo, S. Huang, Y. Wu, H. Wang, H. Wang, and L. Zhang, "Improved electromechanical properties of brominated butyl rubber filled with modified barium titanate," *RSC advances*, vol. 7, no. 59, pp. 37148–37157, 2017.
9. D. Yang, Y. Ni, X. Kong, H. Xue, W. Guo, and L. Zhang, "Enhanced electromechanical properties of natural rubber using highly efficient and cost-effective mussel-inspired modification of tio2 nanoparticles," *Applied Surface Science*, vol. 495, p. 143638, 2019.
10. G. Yin, Y. Yang, F. Song, C. Renard, Z. M. Dang, C. Y. Shi, and D. Wang, "Enhanced electromechanical properties of natural rubber using highly efficient and cost-effective mussel-inspired modification of tio2 nanoparticles," *ACS Applied Materials and Interfaces*, vol. 9, no. 6, pp. 5237–5243, 2017.
11. T. Jose, G. Moni, S. Salini, A. J. Raju, J. J. George, and S. C. George, "Multifunctional multi-walled carbon nanotube reinforced natural rubber nanocomposites," *Industrial Crops and Products*, vol. 105, pp. 63–73, 2017.

12. Y. J. Lee, P. Caspari, D. M. Opris, F. A. Nüesch, S. Ham, J.-H. Kim, S.-R. Kim, B.-K. Ju, and W. K. Choi, "Electrical energy generated by silicone elastomers filled with nanospring-carbon-nanotubes," *Journal of Materials Chemistry C*, vol. 7, no. 12, pp. 3535–3542, 2019.
13. A. Kumar, K. Patra, and M. Hossain, "Silicone composites cured under a high electric field: An electromechanical experimental study," *Polymer Composites*, vol. 42, no. 2, pp. 914–930, 2021.
14. A. Ziegmann and D. W. Schubert, "Influence of the particle size and the filling degree of barium titanate filled silicone elastomers used as potential dielectric elastomers on the mechanical properties and the crosslinking density," *Materials Today Communications*, vol. 14, pp. 90–98, 2018.
15. A. Ziegmann, C. Berner, and D. W. Schubert, "Investigation and modeling of various influencing factors on the dielectric breakdown strength of silicone elastomers," *Materials Science and Engineering: B*, vol. 243, pp. 65–70, 2019.
16. C. Huang, Q. Zhang, J. Y. Li, and M. Rabeony, "Colossal dielectric and electromechanical responses in self-assembled polymeric nanocomposites," *Applied Physics Letters*, vol. 87, no. 18, p. 182901, 2005.
17. M. Mehnert, M. Hossain, and P. Steinmann, "A complete thermo-electro-viscoelastic characterization of dielectric elastomers, part i: Experimental investigations," *Journal of the Mechanics and Physics of Solids*, p. 104603, 2021.
18. R. W. Ogden and D. G. Roxburgh, "A pseudo–elastic model for the mullins effect in filled rubber," *Proceedings of the Royal Society of London. Series A: Mathematical, Physical and Engineering Sciences*, vol. 455, no. 1988, pp. 2861–2877, 1999.
19. A. Dorfmann and R. W. Ogden, "A constitutive model for the mullins effect with permanent set in particle-reinforced rubber," *International Journal of Solids and Structures*, vol. 41, no. 7, pp. 1855–1878, 2004.
20. K. Ghosh, B. Shrimali, A. Kumar, and O. Lopez-Pamies, "The nonlinear viscoelastic response of suspensions of rigid inclusions in rubber: I—gaussian rubber with constant viscosity," *Journal of the Mechanics and Physics of Solids*, vol. 154, p. 104544, 2021.
21. T. Pössinger, C. Bolzmacher, L. Bodelot, and N. Triantafyllidis, "Interfacial adhesion between the iron fillers and the silicone matrix in magneto-rheological elastomers at high deformations," in *Smart Sensors, Actuators, and MEMS VI*, vol. 8763, pp. 480–490, SPIE, 2013.